RSC Advances

ROYAL SOCIETY OF CHEMISTRY

www.rsc.org/advances

Dynamic Article Links ►

Cite this: DOI: 10.1039/c0xx00000x

www.rsc.org/xxxxxx

ARTICLE TYPE

Skutterudites as thermoelectric material: revisited

M.Rull-Bravo,[a] A. Moure,[b] J.F. Fernández,[b] M. Martín-González,*[a]

Received (in XXX, XXX) Xth XXXXXXXXX 20XX, Accepted Xth XXXXXXXXX 20XX
DOI: 10.1039/b000000x

The research on Skutterudites in the last years has contributed to a better understanding of the physical processes which play an important role in enhancing their thermoelectric performance and to the discovery of novel filled compounds, with one of the most promising zT values at intermediate temperatures. Skutterudites are still an ongoing field of research, and an improvement of their efficiencies, stabilities, contacts, industrial scalable fabrication processes and other factors are expected in a near future in order to carry out viable modules for intermediate temperature range applications, such as automobile industry, factories or incinerators. This paper gives a review on the status of research in the field of Skutterudites.

1. Introduction

The consumption habits and the growing need for energy in our world have awoken the interest in alternative energy sources, along with new technologies able to optimize the energy efficiency of traditional routes of fuel combustion. According to calculations, two-thirds of the energy produced for human consumption are wasted as heat.[1] In the more specific case of the automobile, it is calculated that only 25% of the fuel introduced in a car is transformed into useful energy.[2] Within this context, thermoelectricity appears as a viable alternative with a promising future that combines a clean energy source with the possibility of increasing the global energy efficiency [3] (Fig. 1).

The thermoelectric effect is the direct conversion of a temperature gradient into electricity (Seebeck effect) and *vice-versa* (Peltier effect). Therefore, solid state thermoelectric devices mainly possess two important applications: as thermoelectric generators, which are able to generate a voltage potential by applying a temperature difference, or as refrigerators, acting as (micro-) coolers. Thermoelectric generators (TEGs) are capable of converting the waste heat generated by different sources (such as solar irradiation, heat generated in the car exhaust or in industrial processes) into usable electricity. Advantages of these devices are long-term equipments, low environmental impact, mechanical stability and high reliability (without moving parts).[4-5]

The first manufactured TEG devices were thermoelectric-powered radios using a kerosene lamp in Russia in the 1950s,[6] but until the 1990s, the conversion efficiency of these thermoelectric devices was low (ca. 4-6%) and their applications were limited, to space missions, medical applications or laboratory equipment.

Conversion efficiency of electricity generation η is directly governed by Carnot efficiency η_C and the Figure of Merit ($Z\bar{T}$) given by

$$\eta = \eta_C \left[\frac{(1+Z\bar{T})^{1/2} - 1}{(1+Z\bar{T})^{1/2} + \left({}^{T_C}/{}_{T_H} \right)} \right]. \qquad (1)$$

Here, $\eta_C = (T_H - T_C)/T_H$ is the Carnot efficiency, T_H and T_C are the temperatures of the hot and cold sides of the TE legs, respectively, $Z\bar{T}$ is the Figure of Merit of the thermocouple at the average temperature $\bar{T} = (T_H + T_C)/2.$[7]

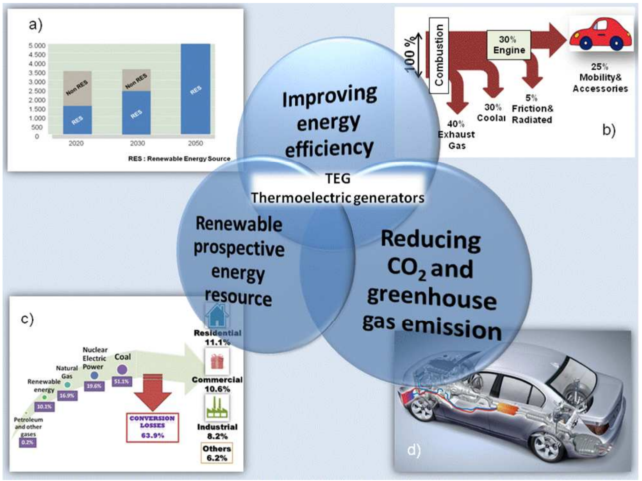

Fig. 1 Characteristics of the electricity generators devices based on thermoelectricity: a) Plan for the European Union called *"Re-thinking 2050"* to obtain 100% of its energy needs with renewable sources by 2050: 31% from wind, 27% from solar PV, 12% from geothermal, 10% from biomass, 9% from hydroelectric, 8% from solar thermal and 3% from the ocean (Source: EREC)[8];b)Typical energy path in gasoline fuelled internal combustion engine vehicle; c) Diagram of the useful consumed and the wasted as heat energy in 2007 in USA (Source: Energy Information Administration Annual Energy Review 2007; d) Prototype of a thermoelectric device used to increase the energetic efficiency and to reduce the CO_2 production in automobiles (Source: BMW).[5]

Cite this: DOI: 10.1039/c0xx00000x

www.rsc.org/xxxxxx

ARTICLE TYPE

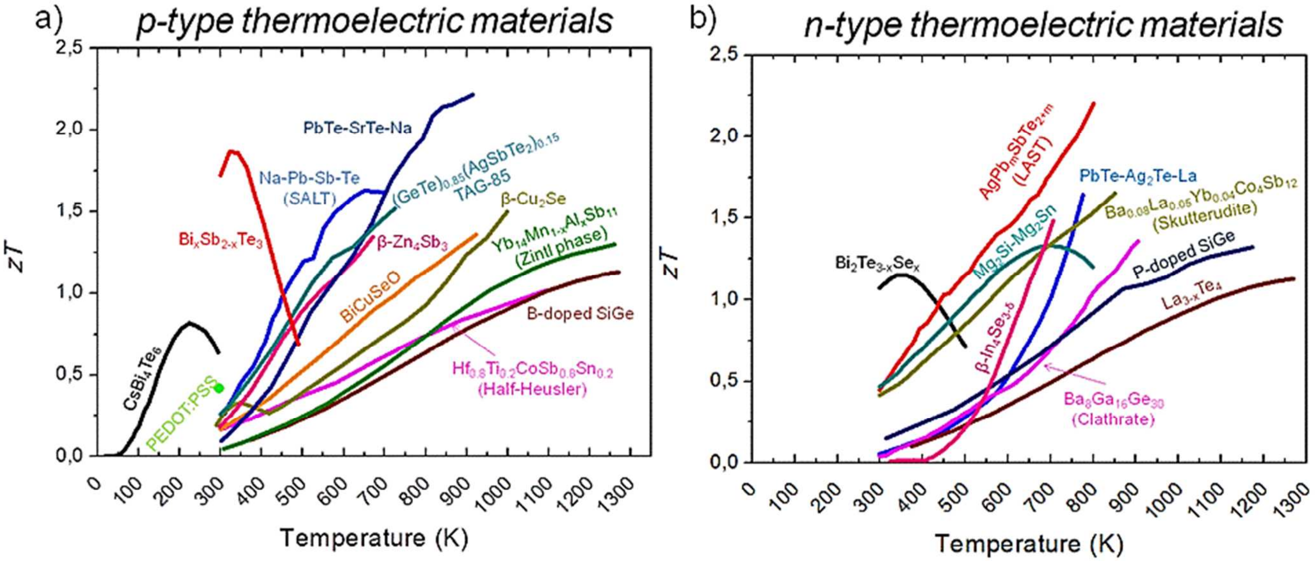

Fig. 2 Summary of some of the best *zT* for bulk thermoelectric materials to date as a function of temperature: a) p-type thermoelectric materials are $CsBi_4Te_6$[9], polymer PEDOT:PSS[10], $Bi_{0.5}Sb_{1.5}Te_3$[11],Na-Pb-Sb-Te (SALT)[12],PbTe-SrTe-Na[13], $(GeTe)_{0.85}(AgSbTe_2)_{0.15}$ + 2%Dy[14], β-Zn_4Sb_3[15], BiCuSeO[16],β-Cu_2Se[17], $Yb_{14}Mn_{1-x}Al_xSb_{11}$ (Zintl phase) [18], $Hf_{0.8}Ti_{0.2}CoSb_{0.8}Sn_{0.2}$ (Half-Heusler compound)[19] and B-doped SiGe alloy[20]. b) n-type thermoelectric materials $Bi_2Te_{3-x}Se_x$ +1%Cu[21], $AgPb_{18}SbTe_{20}$ (LAST)[22], $Mg_2Si_{1-x}Sn_x$[23], β-$In_4Se_{3-\delta}$[24],PbTe-Ag_2Te-La[25], $Ba_{0.08}La_{0.05}Yb_{0.04}Co_4Sb_{12}$ (Skutterudite)[26], $Ba_8Ga_{16}Ge_{30}$ (Clathrate)[27], P-doped SiGe alloy[28] and $La_{3-x}Te_4$[29].

The efficiency of a thermoelectric module depends on different factors, such as the electrical connections, contact resistances and lateral heat losses, but the most critical factor is the material itself. The Figure of Merit (zT) of a thermoelectric material is given by:

$$zT = \frac{S^2\sigma}{k}T, \qquad (2)$$

where S is the Seebeck coefficient, σ is the electrical conductivity, k is the thermal conductivity, and T is the temperature. The product of the square of the Seebeck coefficient and electrical conductivity is called the Power Factor($PF = S^2\sigma$).

In order to manufacture a thermoelectric device with a conversion efficiency closer to other traditional mechanical power generators, a Figure of Merit of ~3 would be necessary.[30-31] Therefore, all efforts is focused on the improvement of the zT, the maximization of the Seebeck coefficient and the electrical conductivity, as well as the reduction of the thermal conductivity. However, the optimization of the aforementioned properties is not trivial, as these properties are interrelated in classical physics, for example, an increase of the Seebeck coefficient implies a decrease of electrical conductivity, and electronic thermal conductivity is related to electrical conductivity via the Wiedemann-Franz law. Thus, a balance among them is required.

The Figure of Merit of state-of-the-art thermoelectric materials *versus* the applied temperature is illustrated in Fig. 2. Until 1960, the most known and studied materials were heavy atom-doped semiconductors, such as Bi_2Te_3, PbTe, Si-Ge or Te-Ag-Ge-Sb, where the values of the Figure of Merit zT close to 1 were reached. These values were not enough to generate an interest at funding agencies to continue research; hence most of the developments were carried out on industrial level until the 90's. As a result, commercial modules based on the Bi_2Te_3 family became the most popular thermoelectric material used for chair heaters, IC chip cooling or portable refrigerators.

For high temperature operation of thermoelectric power generation devices, the most known material until the 80's were Si-Ge alloys. Famous applications for this device were the space probes Voyager 1 and 2, which used a radioisotope thermoelectric generator based on a Si-Ge module[32].

With the publication of new theories about how to increase the efficiency of a thermoelectric device, which predicted efficiencies higher than 15%, and the discovery of new thermoelectric materials with interesting properties, the world focused its attention on this field and several new projects appeared, giving a new impetus to thermoelectricity.

After the 90's, two novel proof-of-principle approaches were presented and thermoelectric field had a re-emergence. These new strategies to improve thermoelectric efficiencies could be summarized by two fundamental aspects: nanostructures and study of new materials based on the "Phonon Glass and Electron Crystal" concept.[33]

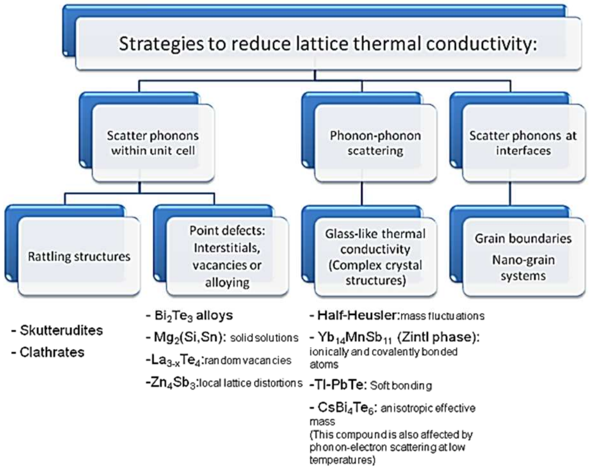

Fig. 3 Different strategies to reduce lattice thermal conductivity, and a few examples of the materials where these effects are better represented.[33]

The first one was based on the effect of reducing the dimensionality of thermoelectric materials by nanostructuration. The thermoelectric performance would be improved through the reduction of thermal conductivity by phonon scattering at the grain boundaries (Rowe, 1981) [34] and possible enhancement of Power Factor by the quantum confinement effect (Hicks and Dresselhaus, 1993). [35]

It was found that this size reduction, upon nanoengineering the materials, significantly decreased thermal conductivity of the network,[36-37] although the second point of the quantum confinement has not been proved yet.

The second approach focused on new complex materials with phonon-glass electron-crystal (PGEC) properties, proposed by Slack.[38-39] The voids in the crystal structure of these materials could be filled with heavy elements atoms, acting as rattlers and increasing the number of phonon scattering centers, hence reducing the lattice thermal conductivity significantly. The main characteristic of these thermoelectric materials is that they can carry the electrical current as a crystal, but behave as amorphous materials with respect to the lattice thermal conductivity. Skutterudites, Clathrates and β-Zn_4Sb_3 phases are among the most known examples.

Recent strategies to improve thermoelectrical systems are focused on decoupling the thermopower factor and the thermal conductivity, through complex nanostructured materials.[40] In order to increase the Power Factor, it is possible to tailor the band structure near the Fermi level, leading to higher effective mass, through doping[41]. However, a compromise between large effective masses and mobilities is required, as well as the optimization of carrier concentration. Furthermore, a main research focus is the reduction of thermal conductivity, creating different phonon scattering at different length scales but maintaining the electron flow.[42]

Fig. 3 summaries the different strategies to reduce lattice thermal conductivity known at the moment and the materials they comprise.[40] Obviously, the same material can be affected by several strategies. These physical phenomena affect not only the phonon scattering, but also the band structure of the material modifying the Power Factor.

Apart from the search for high zT values, research on new thermoelectric materials nowadays focuses on lead and/or tellurium free materials, with good mechanical and thermal stability, formed by cheaper, earth-abundant and less toxic elements and materials with good reproducibility for an easy technological transference to industry.

As can be observed in Table 1, compounds based on bismuth telluride are among the most studied materials at low temperature applications (RT- 400K), due to their high Figure of Merit (best zT of 1.86 at 320K for p-type[11] and 1.15 at 340K for n-type[21]) and good thermal stability. Nevertheless, the main drawback of these families of materials is the scarceness of raw materials.

At high temperatures (>900K), an enormous improvement was reached, achieving Figure of Merits higher than one for almost all the families. Most known materials are shown in Fig. 2: SiGe alloys[20], $La_{3-x}Te_4$[29], Zintl phases ($Yb_{14}Mn_{1-x}Al_xSb_{11}$)[18], new thermoelectric materials called phonon-liquid electron-crystal (PLEC), such as $Cu_{2-x}Se$, which possess low thermal conductivities due to the high mobility of the copper with superionic behavior,[17] and oxides[16]. Oxides emerged due to its promising performance and environmental friendlyness[43]. However, they usually have higher lattice thermal conductivity and lower mobility than other thermoelectrics, due to the strong bonding of light atoms and the high electronegativity of oxygen, respectively. These properties give oxides a major drawback limiting these materials to broaden application.

Compounds based on lead telluride or related families, such as $AgPb_mSbTe_{2+m}$ (called LAST (Lead-Antimony-Silver-Tellurium), $(GeTe)_{1-x}(AgSbTe_2)_x$ (TAGS (Tellurium-Antimony-Germanium-Silver), $Na_{1-x}Pb_mSb_yTe_{m+2}$ (SALT),[12] etc, presented the best Figure of Merit known until now for bulk thermoelectric materials, with values of 2.2 at 915K for p-type PbTe doped with 4% SrTe and 2% Na,[13] 1.6 at 775 K for the n-type doped with Ag_2Te and La,[25] or 2.2 at 800K for the n-type compound $AgPb_{18}SbTe_{20}$ (LAST) for medium range applications (400-800K).[22]

Promising materials for middle temperature applications are magnesium silicide and related alloys,[23, 44-45] superionic phases,[46-47] Half-Heusler compounds[19, 27] and compounds based on PGEC concept, such as Skutterudites[26] or Chlathrates[27]. There are many efforts to enhance the Figure of Merit and the properties and stabilities of these new thermoelectric materials, due to the growing interest in obtaining lead and tellurium-free thermoelectric materials. This attention is related to the restriction of the use of lead and other materials in electrical and electronic equipment in Europe. The two directives from the European Union called *"Waste from Electrical and Electronic Equipment (WEEE)"* and *"Restriction of Hazardous Substances (RoHS)"* took effect in July 2006.[48] More specifically, the use of lead in automotive thermoelectric materials will be prohibited from January 2019. [49]

Major improvements in these lead-free thermoelectric families are expected in the future as well as the transfer of this knowledge to the industry. Other emerging non-toxic families

Cite this: DOI: 10.1039/c0xx00000x

www.rsc.org/xxxxxx

ARTICLE TYPE

Table 1: Summary of some of the best known thermoelectric families: their application temperature range; *zT* values; thermal, mechanical and chemical stability at operation temperature; toxicity/ environmental impact; and the availability of raw materials and possibility of large scale production and device fabrication, according to published data. Color code: green (favorable or safe), red (unfavorable or not-safe), orange (intermediate), question mark no information was found in literature.

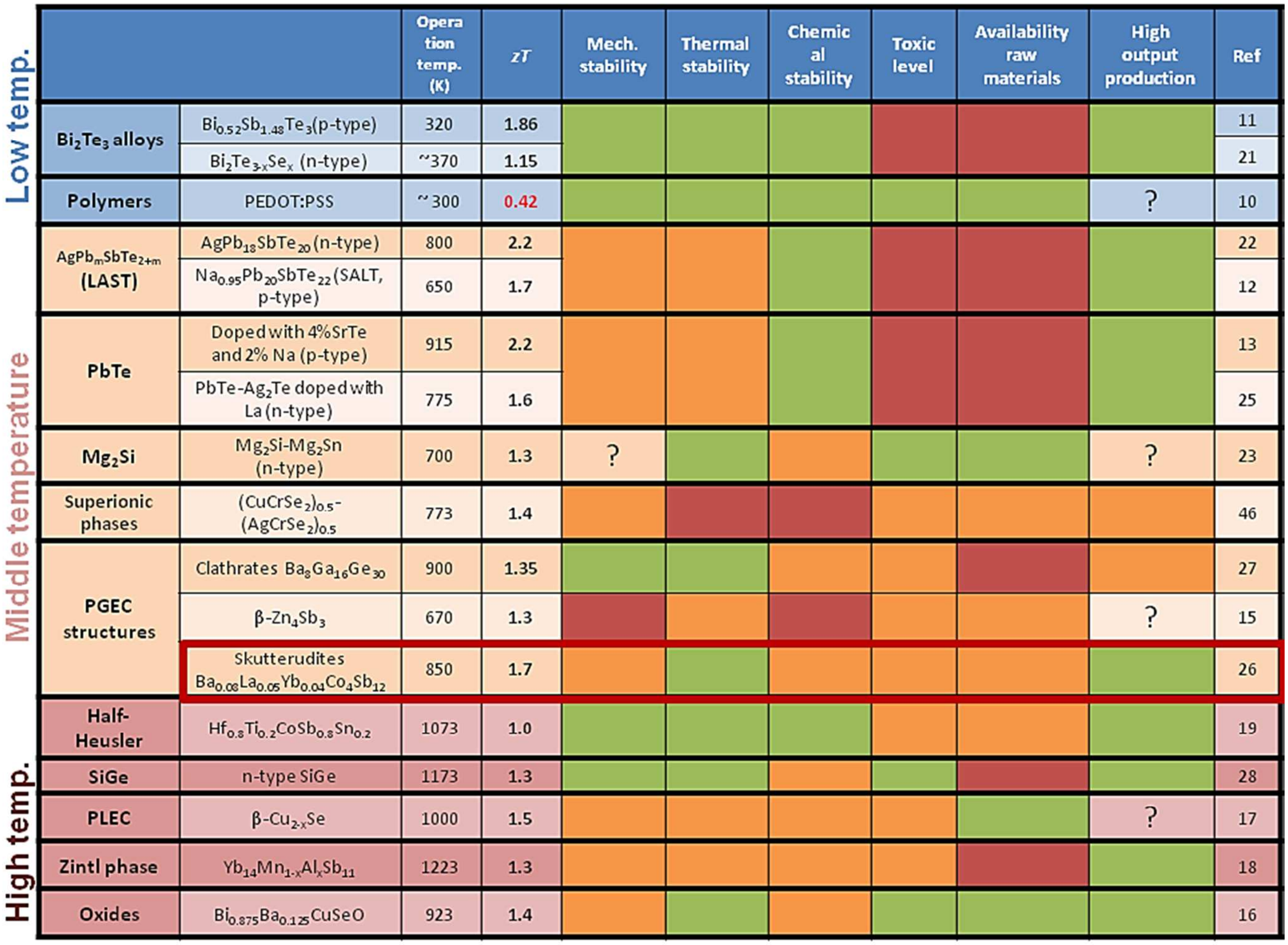

			Operation temp. (K)	*zT*	Mech. stability	Thermal stability	Chemical stability	Toxic level	Availability raw materials	High output production	Ref
Low temp.	Bi_2Te_3 alloys	$Bi_{0.52}Sb_{1.48}Te_3$(p-type)	320	1.86	🟩	🟩	🟩	🟥	🟥	🟩	11
		$Bi_2Te_{3-x}Se_x$ (n-type)	~370	1.15							21
	Polymers	PEDOT:PSS	~300	0.42	🟩	🟩	🟩	🟩	🟩	?	10
Middle temperature	$AgPb_mSbTe_{2+m}$ (LAST)	$AgPb_{18}SbTe_{20}$ (n-type)	800	2.2	🟧	🟧	🟩	🟥	🟥	🟩	22
		$Na_{0.95}Pb_{20}SbTe_{22}$ (SALT, p-type)	650	1.7							12
	PbTe	Doped with 4%SrTe and 2% Na (p-type)	915	2.2	🟧	🟧	🟩	🟥	🟥	🟩	13
		PbTe-Ag_2Te doped with La (n-type)	775	1.6							25
	Mg_2Si	Mg_2Si-Mg_2Sn (n-type)	700	1.3	?	🟩	🟧	🟩	🟩	?	23
	Superionic phases	$(CuCrSe_2)_{0.5}$-$(AgCrSe_2)_{0.5}$	773	1.4	🟧	🟥	🟥	🟧	🟧	🟧	46
	PGEC structures	Clathrates $Ba_8Ga_{16}Ge_{30}$	900	1.35	🟩	🟩	🟧	🟧	🟥	🟧	27
		β-Zn_4Sb_3	670	1.3	🟥	🟧	🟥	🟧	🟧	?	15
		Skutterudites $Ba_{0.08}La_{0.05}Yb_{0.04}Co_4Sb_{12}$	850	1.7	🟧	🟩	🟧	🟧	🟧	🟩	26
High temp.	Half-Heusler	$Hf_{0.8}Ti_{0.2}CoSb_{0.8}Sn_{0.2}$	1073	1.0	🟩	🟩	🟩	🟧	🟧	🟩	19
	SiGe	n-type SiGe	1173	1.3	🟩	🟩	🟧	🟩	🟥	🟩	28
	PLEC	β-$Cu_{2-x}Se$	1000	1.5	🟧	🟧	🟧	🟧	🟩	?	17
	Zintl phase	$Yb_{14}Mn_{1-x}Al_xSb_{11}$	1223	1.3	🟧	🟧	🟧	🟧	🟥	🟩	18
	Oxides	$Bi_{0.875}Ba_{0.125}CuSeO$	923	1.4	🟧	🟩	🟧	🟩	🟩	🟩	16

and earth abundant are sulfosalts[50-51]. Best results were found in tetrahedrites[52-53], with *zT* exceeding unity, 1.13 at 575K[52], due to the low thermal conductivity by their complex crystal structure.

Among thermoelectric materials with high efficiency and lacking the non-desired tellurium or lead, Skutterudites stand out with a promising future. As can be observed in Table 1, all the parameters studied for Skutterudites are favorable or safe and/or intermediate. The elements that comprise them are not highly toxic and relatively abundant. Skutterudites present high *zT* values, and are mechanically and thermally stable. They are currently produced on a large scale.

2. Skutterudites

2.1 Structural parameters and bonds for binary Skutterudites

The Skutterudite is a type of arsenide mineral that was first discovered in Norway in 1845. Its composition is $CoAs_3$ with iron or nickel substituting cobalt. Its general formula is TPn_3 where T is a transition metal and Pn is a pnictogen. Oftedal was the first to describe its structure in 1928[54] as a cubic structure containing 32 atoms with a space group *Im*-3. The unit cell consists of eight cubes of the transition metal (being T=Co, Rh or Ir) occupying the *8c* sites (¼, ¼, ¼), with six of these cubes filled with square planar rectangles of the pnictogen (being Pn=Sb, As or P) occupying the *24g* (0, y, z) sites. (Fig. 4a)

The two remaining voids in the unit cell (*2a* (0, 0, 0) or (½, ½, ½) sites) can be filled by atoms with ionic radii smaller than the cage. The formula describing the unit cell for binary Skutterudites is $\square_2T_8Pn_{24}$, where □ denotes the voids that can be filled with rare earth or alkaline-earth elements. It is more common to describe it as the half of the unit cell $\square T_4Pn_{12}$, which is isoelectronic with 72

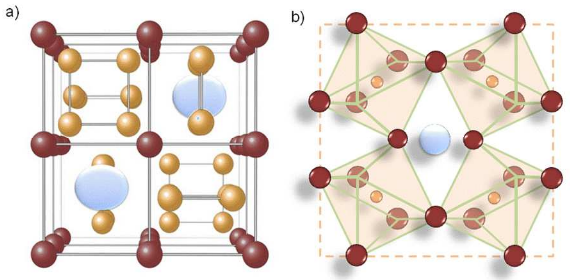

Fig. 4 Unit cell of the Skutterudite, a) described by Oftedal *et al.* in 1928;[54] b) crystalline structure defined by Kjekshus *et al.* in 1974,[55] where the octahedral coordination of the metal atom is drawn. For both images, transition metals are represented by red spheres, pnictogen atoms by yellow spheres and the voids in the structure or the filled atoms by light blue spheres.

valance electrons.

The first assumption of Oftedal, that the distance between the pnictogen atoms were the same ($d_1 = d_2$) and regular octahedral positions for pnictogen atoms, was modified in the 70s, when Kjekshus *et al* experimentally proved that none of the binary Skutterudites satisfied the Oftedal relation $2(y + z)=1$. Therefore, the more precise crystalline structure for Skutterudites would be distorted perovskite-type structure ReO_3, while the pnictogen rings are rectangular and not square. Kjekshus attributed rectangular distortions to the anisotropic environment and the presence of the two voids in the structure per unit cell. (Fig. 4b).

These lattice favor distortions are better understood when the atomic bonds are observed. The nature of the bonds in the Skutterudites is mainly covalent. The distance between transition metal atoms is too large to create a bonding, thus the interactions occur between Pn-Pn (the pnictogen atoms), forming the Pn_4 rings, and T-Pn bondings (the metallic atoms with the pnictogen). The valence electrons configuration of the pnictogen atoms is ns^2np^3 type, giving five electrons to each bond. Two of these electrons are localized in the bonding with the two nearest pnictogen atoms, and the remaining three valence electrons are localized in the bonding with the two nearest metallic atoms. From the perspective of the metallic atom, it contributes with three electrons by bonding with the six neighbor pnictogen atoms, resulting in an octahedral hybridization of the d^2sp^3 orbitals. This generates an octahedral coordination TPn_6, in which the 18-electron rule is fulfilled, 9 given by the pnictogen atoms and 9 from the valence electrons of the metallic atom. This configuration favors the diamagnetism and the semiconductor character of the Skutterudites.

The structural parameters of several binary Skutterudites have been studied, observing in all of them the distortion of the pnictogen squares ($d_1 \neq d_2$). The structure can be defined by the lattice parameter *a*, and the distances between the pnictogen atoms *y* and *z*.

As can be observed in Table 2, increasing the atomic mass of the metal atom also increases the lattice parameter. Similarly, it is shown that the lattice parameters and the void size (R) are larger for the antimony Skutterudites.

Table 2 Structural parameters of binary Skutterudites, based on phosphorus (green), arsenium (violet) and antimony (blue). Data from Kjeshus and Rakke (1974)[55] and Nolas *et al* (1996).[56]

	Lattice constant (Å)	*y (Å)*	*z (Å)*	*d T-Pn (Å)*	*d_1 Pn-Pn (Å)*	*d_2 Pn-Pn (Å)*	*R (void) (Å)*
CoP_3	7.7073	0.3482	0.1453	2.222	2.240	2.340	1.763
RhP_3	7.9951	0.3547	0.1393	2.341	2.227	2.323	1.909
IrP_3	8.0151	0.3540	0.1393	2.345	2.233	2.340	1.906
NiP_3	7.8192	0.3540	0.1417	2.280	2.216	2.283	--
$CoAs_3$	8.2055	0.3442	0.1514	2.337	2.478	2.560	1.825
$RhAs_3$	8.4507	0.3482	0.1459	2.434	2.468	2.569	1.934
$IrAs_3$	8.4673	0.3477	0.1454	2.441	2.456	2.574	1.931
$CoSb_3$	9.0385	0.3351	0.1602	2.520	2.891	2.982	1.892
$RhSb_3$	9.2322	0.3420	0.1517	2.621	2.807	2.917	2.024
$IrSb_3$	9.2503	0.3407	0.1538	2.617	2.850	2.943	2.040

2.2 Skutterudites based on $CoSb_3$

The most studied Skutterudites for thermoelectric materials are those based on antimony, due to their high mobility, high atomic masses, low electrical resistivity and good Seebeck coefficients. More specifically, Caillat *et al* found a high mobility 3445 $cm^2V^{-1}s^{-1}$, and a charge concentration of 4.10^{17} cm^{-3} at room temperature for single crystals of $CoSb_3$.[57]

$CoSb_3$ holds very promising thermoelectric properties, with a high power factor ($30 \mu W/cm^{-1}K^{-1}$) and a high Seebeck coefficient ($200 \mu V/K$). However, its thermal conductivity is also high (8.9 $Wm^{-1}K^{-1}$ at 300K) and therefore most efforts are focused on reducing this value to achieve a high *zT*.[58].

Best Figure of Merit for undoped $CoSb_3$ was 0.17 at 610K.[59] This *zT* value was achieved through nanostructuration and hot pressed compaction. However, depending on the synthesis and compaction technique, thermoelectric properties of undoped $CoSb_3$ changes drastically, exhibiting p-type or n-type conductivities, and sometimes, both behaviors, changing from n to p-type at high temperatures. This n-type behavior is usually related to impurities and/or Sb-deficient samples.[60-64]

The approaches used to improve the efficiency of $CoSb_3$ can be divided in:

- Modification of the crystalline structure by: a) the filling of guest atoms in the structure voids, or b) doping at cobalt or antimony sites to generate defects.
- Nanostructuration and nanocomposites, where the defects, grain boundaries and interfaces help to increase the phonon scattering in order to reduce the thermal conductivity.

2.2.1 Filled Skutterudites

This approach always leads to n-type Skutterudite.

Within the approaches to reduce the lattice thermal conductivity of the compounds based on $CoSb_3$, the introduction of filler atoms in the voids of the crystalline structure is one of the most studied.

According to the theory of the PGEC materials proposed by Slack at the early 90s,[38-39] these materials must have a large unit cell, with heavy atoms in their structure, small differences in the electronegativity of the constituent atoms and a high charge mobility. Slack and Tsoukala[65] postulated that the guest atoms in the voids act as independent oscillators (rattle effect), interacting with the normal phonon modes and decreasing in this way the thermal phonon conductivity in filled Skutterudites. Rattlers not only affect to thermal conductivity, but also improve electrical conductivity, because fillers generally are electropositive elements, albeit having a negligible effect on the band structure, thus the Seebeck coefficient is not modified.

Traditionally, the role of the filler was associated with the additional and independent resonant scattering mode introduced by the weak interactions between the filler and the host structures. [65-66] This rattling behavior was also supported by the observation of localized modes in two experiments using heat-capacity and inelastic-neutron scattering measurements.[67-68] However, there is a controversy over this point. The rattler model was challenged by the calculations of interaction between host and filler done by Feldman *et al* [69] (where they showed that the rattler has a strong harmonic potential associated with the mobility of the filler in its cage) and the experiments performed in La-and Ce-filled Fe_4Sb_{12}-type Skutterudites [70] (where the coherent propagation of the filler-related phonons was not easy to be interpreted by the existing theory).

In general, it was accepted that the introduction of the filler modifies the phonon dispersion processes for fully filled Skutterudites. Li and Mingo have reached the conclusion [71] by using *ab initio* calculations that the reduction of the thermal conductivity in filling Skutterudites can be due to an increase of anharmonic scattering rates, with a contribution from the reduction of group velocities (that is, the phonon lifetime reduction).

First experiments filling the Skutterudites were performed by Jeitschko and Braun, successfully obtaining different lanthanum filled- Skutterudites.[72]

It is important at this point to define two types of different filled Skutterudites:

- Binary isoelectronic Skutterudites, which have filled icosahedron voids of the structure (see Fig. 4a). This type of compounds has a limit of filling fraction and always has n-type conductivity.
- Non-isoelectronic Skutterudites, whose structure is stabilized by the electrons provided by the guest atom. Examples of the first group are filled Skutterudite, such as the $Ba_{0.08}La_{0.05}Yb_{0.04}Co_4Sb_{12}$ compound[26] and for the second group the $LaFe_3CoSb_{12}$ or $CeFe_{4-x}Co_xSb_{12}$ Skutterudites.[73-75] This second group will be revised in the section on filled and doped Skutterudites.

The limit of the filling fraction depends on both the radius of the void in the structure and on the ionic and the valence state of the guest ion. Chen *et al* proved that the stability range of r_{ion}/r_{cage} is between 0.6 and 0.9.[76] This stability range depends mainly on the oxidation state (n) of the introduced atom in the following manner

$$Y_{max}=r_{ion}/r_{cage} - 0.086n - 0.24 \qquad (3)$$

Considerable research has been conducted in fillings with alkaline metals (Na, K, Rb), alkaline-earth (Ca, Sr, Ba), elements of the XIII group (In, Tl) and rare earth elements (La, Ce, Pr, Nd, Sm, Eu and Yb). Shi *et al* summarized in their review the theoretical and experimental filling fraction limits.[77] They found that partially filled Skutterudites are very sensitive to the difference of electronegativity between the antimony and the guest atom. They also established a simple rule to predict the thermodynamic stability of filled Skutterudites with $R_yCo_4Sb_{12}$ composition: $\chi_R - \chi_{Sb} > 0.8$, with χ_R and χ_{Sb} being the electronegativity of the filler atom and antimony, respectively.

The values of the thermal conductivity have been reduced down to values lower than 2 $Wm^{-1}K^{-1}$, increasing the Figure of Merit, due to the introduction of the guest atoms and the optimization of the concentration... The best results were obtained for samples with Yb, proving that rare earth elements are very efficient by introducing additional vibration modes at low frequencies and scattering those phonons.[78] *zT* values of 1.26 at 800K were obtained for $Yb_{0.2}Co_4Sb_{12.3}$, achieving some of the lowest thermal conductivities (1.8 $Wm^{-1}K^{-1}$) at room temperature. [79] Other promising values have been obtained with alkaline (Na^{80},K^{81} or Li^{82}) and alkaline-earth metals (Ba^{83}, Ca^{84} or Sr^{85})

It seemed that a limit was reached in the efficiency when only introducing a unique guest atom. However, the influence of multifilling was not clarified until the study of Yang *et al*,[78] who predicted a higher phonon scattering by choosing two guest atoms with a difference of resonance frequencies as high as possible.

One of the first contributions which introduced two different guest atoms was published by Lu *et al*. Values of 1.81 $Wm^{-1}K^{-1}$ of thermal conductivity were achieved for the $Ce_{0.1}La_{0.2}FeCo_3Sb_{12}$ Skutterudite. However, the electrical conductivity was low and values of *zT* of 0.6 at 773K were accomplished.[86]

Finally, the filling by three different guest atoms was also studied, giving the best Figure of Merit up to now for n-type Skutterudites with values of 1.7 at 850K for the $Ba_{0.08}La_{0.05}Yb_{0.04}Co_4Sb_{12}$ compound[26], 1.8 at 800K for $Sr_{0.07}Ba_{0.07}Yb_{0.07}Co_4Sb_{12}$ after HPT treatment[87] and 1.9 at 835K for $Sr_{0.09}Ba_{0.11}Yb_{0.05}Co_4Sb_{12}$.[88]

Fig. 5 summarizes best *zT* values for one, two or three guest atoms into the Skutterudite structure and its temperature application.

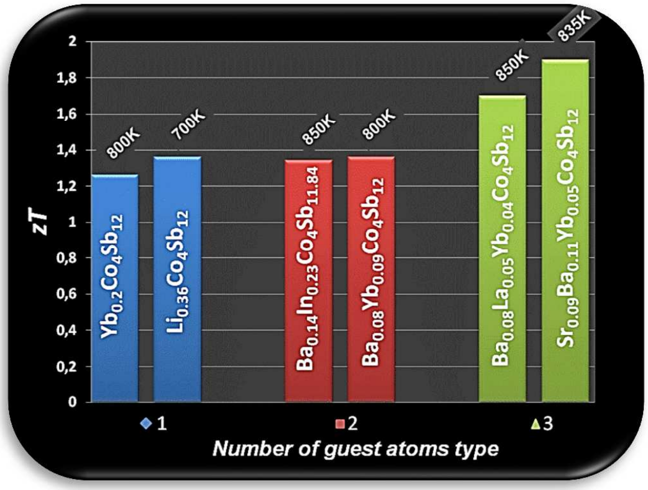

Fig. 5 Best *zT* values obtained with the different guest atoms for n-type Skutterudites: $Yb_{0.2}Co_4Sb_{12.3}$[79], $Li_{0.36}Co_4Sb_{12}$[82], $Ba_{0.14}In_{0.23}Co_4Sb_{11.84}$[89],

$Ba_{0.08}Yb_{0.09}Co_4Sb_{12.12}$[90], $Ba_{0.08}La_{0.05}Yb_{0.04}Co_4Sb_{12}$[26] and $Sr_{0.09}Ba_{0.11}Yb_{0.05}Co_4Sb_{12}$[88]

2.2.2 Doped and filled Skutterudites

This type of approach is normally used for n- and p-type Skutterudites.

A different phenomenon is observed for the type p or n doped Skutterudites. In this case, part of the Co and/or Sb are substituted by a similar element with a higher number of electrons, acting as donors and giving rise to n-type conduction, or by an element with a lower number of electrons, generating holes and giving rise to p-type conduction. It has been proved that doping levels even lower than 1% strongly influence the electrical properties of the material.

Doping has often been considered to improve only the Power Factor. However, recent studies prove that doping can positively influence the reduction of the thermal conductivity.[91] These point defects create strong phonon scattering by atomic mass fluctuation and size strain, leading to reduced thermal conductivity and improved *zT* .[92]

N-type doped Skutterudites

Typical donor doping of $CoSb_3$ to obtain n-type Skutterudite are Ni, Pd or Pt, [93-94] substituting at the cobalt sites, or Te and Se substituting at the antimony sites.

A strong relationship between dopant concentration and electrical properties was established. The elements with higher mass do not only have an influence on the power factor, but also decrease the thermal conductivity due to point lattice defects that favour phonon scattering. This relationship was observed experimentally with the best result being the doped 5% Pd and 5% Pt Skutterudite, with a *zT* of 0.9 at 750K.[95] Anno *et al*[93] reported the strong influence of nickel on the electronic properties of $CoSb_3$ due to electron-phonon interactions. However, Ni-doped Skutterudites values of *zT* are low in comparison to Pd or Pt. The best value in the literature was 0.7 at 775K for the composition $Co_{0.8}Ni_{0.2}Sb_3$. This value was accomplished by introducing pores in the nanostructured bulk.[96]

It has been proved that the thermal conductivity reduction is more effective with doping in the pnictogen ring, as it dominates the spectrum of phonon thermal conductivity.[69, 97]However, single doping at Sb sites with Te has certain disadvantages, as the Te^{4+} gives an extra electron that saturates the negative charges, thus decreasing the mobility. Despite this, the solubility limit of tellurium in the $CoSb_{3-x}Te_x$ structure is approximately x=0.15. *zT* values of 0.93 for x=0.15[98] and 0.95 for x=0.2[99] were obtained at a temperature of 800 K, approximately.

Recent studies proved the efficiency of double doping in these materials. The solubility limit of tellurium in the structure increases to x=0.2, with a higher scattering by point defects, substituting with Te and other element to compensate the charge (Ge or Sn, for example). The bonding and symmetry of the rings were also altered, leading to changes in the phonon vibration spectrum. As a consequence, the thermal conductivity drastically dropped. Values of *zT* of 1.1 at 800K for $CoSb_{2.75}Ge_{0.05}Te_{0.20}$ [100] and for $CoSb_{2.75}Sn_{0.05}Te_{0.20}$ at 820K were obtained. [91]

Some studies were carried out on n-type Skutterudites doped in both Co sites (with nickel or iron) and Sb sites (with tellurium). The highest *zT* value achieved for double-doped Skutterudite was 1.3 at 820K for $Fe_{0.2}Co_{3.8}Sb_{11.5}Te_{0.5}$, using a special technique combining high pressures with torsion.[101] Doping the Skutterudite with tellurium and nickel, the highest values was 0.65 at 700K for $Co_{0.92}Ni_{0.08}Sb_{2.988}Te_{0.012}$.[102-103]

Table 3 Best *zT* values for n-type doped Skutterudites and its synthesis methods and references. Units for *k* [$Wm^{-1}K^{-1}$]

Compound	***zT***	***k***	**Methods**	**Reference**
$\mathbf{Co_{0.8}Ni_{0.2}Sb_3}$	**0.7** at 775K	2.8	MA+HP	*He et al*,2008[96]
$\mathbf{Co_{3.8}Ni_{0.2}Sb_{12}}$	**0.6** at 800K	~ 3	MA+ SPS	Zhang *et al*,2008[109]
5%Pd and 5%Pt doped $\mathbf{CoSb_3}$	**0.9** at 750K	~ 3	MAG+ HP	Tashiro *et al*, 1997 [95]
$\mathbf{CoSb_{2.75}Sn_{0.05}Te_{0.2}}$ **(M=Si,Ge,Sn,Pb)**	**1.1** at 823K	2.0	HEBM+ SPS	Liu *et al*, 2008[91]
$\mathbf{Co_4Sb_{11.5}Te_{0.5}}$	**0.72** at 850K	4	MAG+SPS	Li *et al*, 2005[110]
$\mathbf{CoSb_{2.85}Te_{0.15}}$	**0.93** at 820K	3	HEBM+ SPS	Liu *et al*, 2007[98]
$\mathbf{Co_4Sb_{11.4}Te_{0.6}}$	**0.95** at 800K	3.6	MAG+ SPS	Duan *et al*,2012 [99]
$\mathbf{CoSb_{2.85}Te_{0.15}}$	**0.98** at 820 K	3.5	SHS + PAS	Liang *et al*, 2014[111]
$\mathbf{CoSb_{2.75}Ge_{0.05}Te_{0.2}}$	**1.1** at 800K	3	MAG+ SPS	Su *et al*, 2011[100]
$\mathbf{Co_8Sb_{23.25}Sn_{0.25}Te_{0.75}}$	**0.78** at 700K	2.58	RF+Annealing	Mallik *et al*, 2008[112]
$\mathbf{Co_{0.92}Ni_{0.08}Sb_{2.97}Te_{0.03}}$	**0.65** at 680K	3.5	CS+HP	Stiewe *et al*, 2005[103]
$\mathbf{Co_{0.92}Ni_{0.08}Sb_{2.988}Te_{0.012}}$	**0.65** at 700K	~3.5	CS+HP	Bertini *et al*,2003[102]
$\mathbf{Co_{3.9}Ni_{0.1}Sb_{11.5}Te_{0.4}Se_{0.1}}$	**1.1** at 725K	3	MAG+ SPS	Xu *et al*, 2014[105]
$\mathbf{Co_{23.87}Sb_{73.88}Pd_{1.125}Te_{1.125}}$	**0.95** at 873K	3.5	MQG+ HP	Chitroub *et al*, 2009[104]
$\mathbf{Fe_{0.2}Co_{3.8}Sb_{11.5}Te_{0.5}}$	**1.3** at 820K	2.8	MQG + HP+HPT	Mallik *et al*, 2013[101]

MA: Mechanical Alloying; **MAG**: Melting, Annealing and Grounding; **CS**: Chemical Synthesis; **MQG**: Melting, Quenching and Grounding; **HEBM**: High Energy Ball Milling; **SHS:** Self-propagating-High-temperature-Synthesis; **HP**: Hot Pressing; **SPS**: Spark Plasma Sintering; **PAS**: Plasma activated sintering ; **HPT**: High-Pressure Torsion; **RF**: Radio Frequency

The efficiency significantly increased to values of 0.95 at 873K for the $Co_{23.87}Sb_{73.88}Pd_{1.125}Te_{1.125}$ compound doping with palladium instead of nickel..[104] Even better results were obtained with double doping at antimony site, for example, *zT* of 1.1 at 725K for $Co_{3.9}Ni_{0.1}Sb_{11.5}Te_{0.4}Se_{0.1}$.[105]

The thermoelectric properties noticeably improved by combining doping with filling, , increasing the frontier of the *zT* values to levels higher than 1.s Examples are the $Ba_{0.3}Ni_{0.05}Co_{3.95}Sb_{12}$ compounds with *zT* of 1.2 at 800K, [106] $Ca_{0.18}Co_{3.97}Ni_{0.03}Sb_{12}$ with *zT* of 1 at 800K[107] or $Ca_{0.07}Ba_{0.23}Co_{3.95}Ni_{0.05}Sb_{12}$ with *zT* of 1.2 at 775 K. [108]

Some of the best values are summarized in Table 3.

P-type doped Skutterudites

The first known compounds with high Figures of Merit were the ones partially or totally doped with Fe at the Co sites. As it was previously stated, they are not isoelectronic compounds, thus it is necessary to introduce filler atoms to stabilize the structure.

Therefore, some examples of doping with iron confirmed that only doping with acceptor dopants was less effective, presenting Figure of Merits < 0.5.[109, 113-114]

The first promising results were reported by Morelli *et al*., who could reduce the thermal conductivity up to 10 times in the $Ce_yFe_{4-x}Co_xSb_{12}$-based compound, where x=0.[115] To achieve the charge compensation, this compound has metallic-type conductivity as Cerium is in a +3 oxidation state, rather than +4.

For p-type Skutterudites, scarce improvements have been achieved with respect to the first results with the $CeFe_{4-x}Co_xSb_{12}$ compound.[75] However, this value has never been reproduced and verified by other laboratories. The highest reproduced *zT* value was achieved by Tang *et al* with a *zT* of 1.1.[116]

Recent approaches to enhance p-type Skutterudite thermoelectric properties focused on three aspects: first, the introduction of heavy elements such as Bi[117], second, the use of 4*d*/5*d* transition metals to form light valence band Skutterudites and enhance the Power Factor[118-119] and third, the increase of phonon scattering by multi-filling, such as mischmetal (Ce-50.8%, La-28.1%, Nd-16.1% and Pr-5.0%)[120] and didymium (Pr-4.76% and Nd-95.24%).[88, 121-123]

The scarcity of having high reproducible p-type values, together with the low stability, is one of the major limitations to high module efficiency based on Skutterudites.

Table 4 Best *zT* values for p-type doped Skutterudites and its synthesis methods and references. Units for *k* [$Wm^{-1}K^{-1}$]

Compound	*zT*	*k*	Methods	Reference
$\mathbf{LaFe_3CoSb_{12}}$	**0.8** at 750K	1.6	MAG + HP	Sales *et al*,1996 [73]
$\mathbf{CeFe_{4-x}Co_xSb_{12}}$	**1.4** at 900K		MAG	Fleurial *et al*,1996[75]
$\mathbf{Ce_{0.12}Fe_{0.71}Co_{3.29}Sb_{12}}$	**0.8** at 750K	2.5	MAG + PAS	Tang *et al*, 2001 [124]
$\mathbf{Ce_{0.28}Fe_{1.5}Co_{2.5}Sb_{12}}$	**1.1 at 750K**		SSR + PAS	Tang *et al*, 2005[116]
$\mathbf{CeFe_3CoSb_{12}}$	**0.87** at 800K	1.28	MAG + SPS	Qiu *et al*,2011[125]
$\mathbf{Yb_{0.25}La_{0.60}Fe_{2.7}Co_{1.3}Sb_{12}}$	**0.99** at 700K	1.8	MAG + SPS	Zhou *et al*, 2013[126]
$\mathbf{DD_{0.65}Fe_3CoSb_{12}}$	**1.2** at 800k	2.4	MA + HP	Rogl *et al*, 2009[127]
$\mathbf{DD_{0.76}Fe_{3.4}Ni_{0.6}Sb_{12}}$	**1.2** at 800K	2.8	MA + HP	Rogl *et al*, 2010[121]
$\mathbf{DD_{0.7}Fe_{2.7}Co_{1.3}Sb_{11.8}Sn_{0.2}}$	**1.3** at 780K (after HPT **1.45** at 850K)	1.9	MQA + HP + (HPT)	Rogl *et al*, 2015[122]

SSR: Solid-state reaction; **MA:** Mechanical Alloying; **MAG:** Melting, Annealing and Grounding; **MQA:** Melting, Quenching and Annealing; **HP:** Hot Pressing; **SPS:** Spark Plasma Sintering; **PAS:** Plasma activated sintering; **HPT:** High-Pressure Torsion

2.2.3 Skutterudites with nanoparticle inclusions

An efficient way to reduce the thermal conductivity is via grain boundaries and nano-inclusions. Several studies were carried out in this direction introducing different kinds of materials in the nanostructured thermoelectric matrix, usually insulators, to produce a more effective scattering. For example, nanoparticles of ZrO_2 [128], PbTe [129], C_{60} [130] or CeO_2 [131] were introduced. However, the thermoelectric properties could not be improved using this method. Interestingly, different mechanisms were observed for these types of compounds, besides the microstructures and nanocomposite formations enhanced the phonon scattering together with the rattle effect or the material doping. Fu *et al* found core-shell microstructures in compounds doped with 2% of Ni, increasing *zT* to 1.07 at 723K [132] or the *in-situ* formation of nanoislands of InSb in the $In_{0.2}Ce_{0.15}Co_4Sb_{12}$ nanocomposite, that improved *zT* up to 1.43 at 800K [133] through a reduction in thermal conductivity. The formation during the synthesis process of Yb_2O_3 particles, located at the grain boundaries, increases the Figure of Merit of the $Yb_{0.25}Co_4Sb_{12}/Yb_2O_3$ nanocomposite from a *zT* of 1 for $Yb_{0.2}Co_4Sb_{12}$ [134] up to a *zT* of 1.3 at 850K [135], at the same conditions. Another example is the formation of GaSb nano-inclusions for the nanocomposite $Yb_{0.26}Co_4Sb_{12}/0.2GaSb$, with a *zT* of 1.45 at 850K [136]. These nano-inclusions within the matrix were favoured by the synthesis method and the later compaction by sintering assisted by plasma pulsed current.

2.2.4 Nanostructuration

Until now, improvements in the Figure of Merit that have been explained in this work are in relation to the composition and structure of the Skutterudite. However, other important factors that have been recently studied are the new methods of material synthesis, the processing of nanostructured powder, and the routes to compact it while maintaining the nanostructuration in dense bulk materials.

Zheng *et al* showed the theoretical results that proved the decrease the thermal conductivity of $CoSb_3$ by reducing the grain size to values lower than 500 nm in diameter [137]. This was further corroborated by Toprak *et al*, achieving binary $CoSb_3$ Skutterudites with thermal conductivity values lower than 1.5 $Wm^{-1}K^{-1}$ for grain sizes lower than 200nm [138].

New synthetic methods have been studied for the material nanostructuration,, for example, melting-quench-annealing [110, 133, 139], melt-spinning [140-142], microwaves [114, 143], High pressure and High Temperature Techniques (HPHT) [82] or chemical methods [59], among others.

One of the rising techniques is the high energy milling [144], as it makes it possible to obtain the nanostructured material at low processing temperatures, pressures and times [145-147].It has been proved that Hot Pressing (HP), High-pressure Torsion (HPT) or Sintering assisted by Plasma current (SPS) are adequate techniques to maintain the nanostructuration and to obtain the bulk material for material compaction. Mi *et al* [148]studied the behaviour of the same Skutterudite material under different synthesis and compaction techniques, reporting the best results by chemical routes and SPS with a *zT* of 0.6. The *zT* was 0.5 with chemical routes and HP, while the *zT* result was less than 0.1 by melting and Hot Pressing. The importance of the compaction technique for thermoelectric properties was corroborated by Rogl *et al*, who observed a reduction in thermal conductivity up to 40% in the same Skutterudite sample performed by Hot Press or HP together with HPT, and an increment of 20% in the *zT*

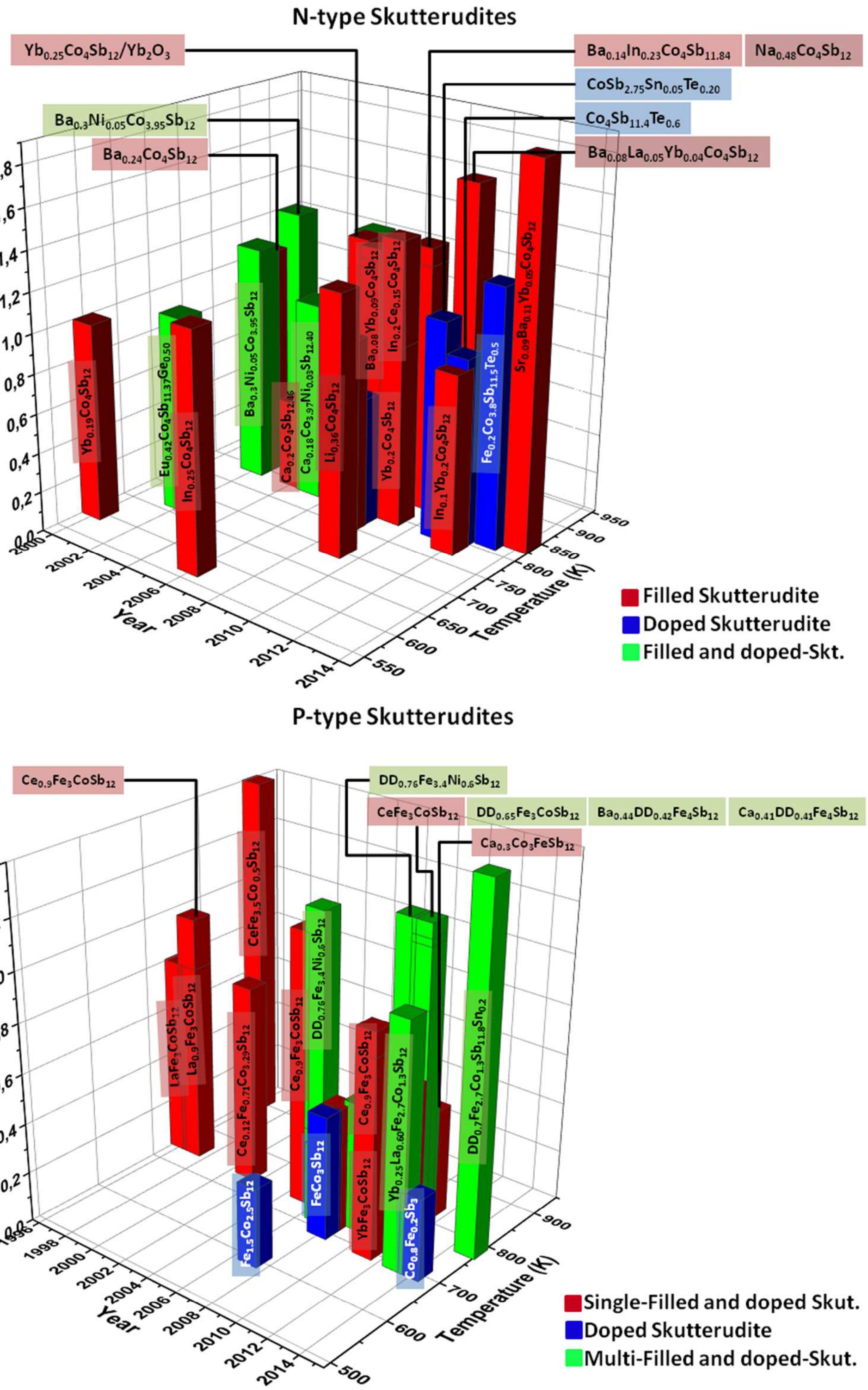

Fig.6 Summary of the best *zT* results fora) n-type doped and/or filled Skutterudites and b) p-type doped and/or filled Skutterudites, depending on the year of publication and operation temperature (K). Only some examples of compounds were plotted in the graph for the sake of clarity.

.

value.[149-150] This technique is quite novel and the values need to be reproduced by other laboratories. In any case, it seems that the obtained *zT* values could be affected by the cyclability of the material.[149]

Significant advances have been made in the last years, and important goals have been achieved in Skutterudite material. Best *zT* results for doped and/or filled Skutterudites are shown in Fig.6. However, further enhancements in the material performance are still to come in order to achieve *zT* values of 2 and higher. Future work to improve Skutterudites can be divided into the following fundamental aspects:

– *N-type filled Skutterudites* show lower lattice thermal conductivities, due to the influence of filling, but further reduction is still expected based on the concept of minimum thermal conductivity. Some approaches to enhance thermoelectric properties of these materials could be based on solid solutions with $RhSb_3$ or $IrSb_3$[151-152] or new fillers, for example. Although the price should be also take into account. Recent studies at high pressures indicated that new elements, breaking the electronegativity rule, could be introduced in the voids, such as Mg[153] or I, reaching even lower thermal conductivities of 0.79 $Wm^{-1}K^{-1}$, [154] which opens a wide range of possibilities in this field. Further improvements in *zT* for N-type Skutterudites should also focus on enhancing the Power Factor, considering how to improve the Seebeck coefficient without sacrificing electrical conductivity using band structure modulation, quantum effect, energy filtering, etc.

– *P-type Skutterudites* show low mobility and bipolar thermal conductivity. These lead to lower Figure of Merits than for the n-type. Band structure modification (increase of band degeneracy, adjustment of band mass) and suppression of bipolar conduction at elevated temperatures are two possible directions.[119] Moreover, an in-deep study on the thermal and mechanical stabilities, especially in p-type Fe-based Skutterudites is also required to enhance the efficiency in the Skutterudite-based thermoelectric devices for commercial applications. [155] Some improvements which have been achieved in strength and fracture toughness, were through the addition of carbon fibers[156], including nanoinclusions[157], or using new synthesis and processing techniques such as melting-spun.[158]

– Finally, *for both type of doping*, new rapid production methods which improve thermoelectric properties through nanostructuration and reduce the synthesis period with the purpose of increasing mass production and open the door for large-scale industrial applications. [111, 145, 149]

2.2.5 Thermoelectric devices based on Skutterudites

Nowadays, most commercial thermoelectric devices are based on Bi_2Te_3 for low temperature applications. The development of a Skutterudite module for middle range temperatures in internal combustion engines, industrial furnaces or incinerators would be of great interest for the industry. As already presented, great improvements have been achieved in the Figure of Merit of Skutterudite materials.

However, a systematic work on the thermal stability of p-type Skutterudites is necessary in order to obtain the maximum efficiency in the Skutterudite-based devices, due to the fact that Fe-based Skutterudites are thermally less stable than $CoSb_3$-based compounds. For this reason, Skutterudite modules generally use Co-rich p-type Skutterudites, with lower *zT* than Fe-rich compositions, instead of Fe doped. Thus, lower efficiencies are achieved in devices nowadays and no commercial devices are available yet.[159]

Additionally, it is necessary to study other factors related to the fabrication of devices, for example, thermal expansion coefficients of the p and n-type legs, minimizing device heat losses, optimizing the electric and thermal conductivity of contacts and the stability under thermo-cycling, to cite some.

Several requirements need to be fulfilled with regard to electrical interconnections joining the p- and n-legs: thermal stability under operating conditions, oxidation resistance, low electrical resistivity, high thermal conductivity, and a thermal expansion coefficient close to those of the p- and n-legs. Rogl *et al* performed a study of thermal expansion of different Skutterudites in order to reduce thermal stress at the joining interface [160]. They realized that these coefficients varied depending on the doping or filling material. The average thermal expansion coefficient (α_m) for doped samples (MT_4Sb_{12}, T=Fe,Co,Ni)) was $11.29*10^{-6}$ K^{-1}, while the average coefficient for filled Skutterudites (MCo_4Sb_{12}) was $8.59*10^{-6}$ K^{-1}.Several studies have been performed with metallic layers, such as Cu [161], Ti [162] or Ni[163], and $W_{80}Cu_{20}$ was found to be an excellent match for $CoSb_3$ legs due to a similar thermal expansion coefficient [164]. However, interdiffusion and chemical reactions of materials at the interfaces are still a not deeply explored field in literature. Joining techniques are also crucial for the design and output power of Skutterudite devices. Possible joining technologies include brazing (high temperature soldering)[161] and spark plasma sintering. [164]

Other important factors in order to obtain a long-durability device involve the thermal stability of the material. One important factor is the sublimation of the antimony resulting in the decomposition of the alloy and the other is the oxidation of $CoSb_3$ when exposed to air at high temperatures. Antimony has a sublimation temperature of 900 K, approximately. Different studies about the stability of $CoSb_3$ and thermal duration showed a weight loss of $CoSb_3$ material between 850 K and 1000 K under vacuum, in agreement with this sublimation temperature, and the formation of secondary phases such as $CoSb_2$ and CoSb.[165] A decline in its thermoelectric properties was observed after a thermal duration test in vacuum for 16 days. Caillat *et al* and Snyder *et al* also reported a starting temperature of decomposition at 848 K and suggested that decomposition was controlled by the antimony diffusion.[166]

Additionally, oxidation behaviour studies at high temperatures in air were performed to understand the degradation of the material under these conditions and the effect on thermoelectric properties. Leszczynski *et al* [167] determined the temperature of oxidation at 653 K and confirmed the main three oxide phases, which were observed in other studies, $CoSb_2O_4$, $CoSb_2O_6$ and α-Sb_2O_4 [168-170] Thermoelectric performance of Skutterudites decreased, especially the electrical conductivity, due to cracks appearing between the $CoSb_3$ interface and the oxide layer.

Protective coating or encapsulation is necessary in order to suppress oxidation and sublimation. This kind of coating should possess low electrical and thermal conductivity, in order to prevent heat losses, good adhesion to the substrate, chemically inert and matching thermal expansion coefficient with the Skutterudite [171]. Some examples are Mo/SiO$_x$ multilayer film [172], composite glass [173-174] or Al$_2$O$_3$. [171] The inorganic-organic hybrid silica is the best approach to obtain a reliable method for device engineering in order to coat Skutterudite material so far.

On the other hand, some experiments of encapsulation by metal enclosure were performed with some thermoelectric materials [175], although further research is still needed.

The fabrication of thermoelectric modules from new materials is a difficult task, but the low cost and good performance of Skutterudites at middle temperatures make them some of the most promising materials for waste heat recovery and many efforts are being made to achieve better efficiencies in these devices [176-177].

Several studies were performed in order to calculate the viability to generate modules. Factors such as manufacturing and system costs and the commercial feasibility were explored [155, 178-180]. LeBlanc *et al* performed an in-depth work on cost considerations for thermoelectrics, taking into account raw material prices, system component costs and manufacturing costs, as well as the optimized geometry in order to improve the thermal and electrical module performance [181]. Fig. 7 shows the system cost of different bulk thermoelectric materials for ΔT=725 K, and their maximum Figure of Merit at lab scale. Skutterudites appear to have low costs in comparison with other families, with the final cost being less than €5.5/W. This is due to the high Figure of Merit and the optimization in the material used for the module (low fill factor and low length). However, further improvements have to be done in order to reduce price per W, as well as in order to increase the efficiency through finding good electrical and thermal contacts and new designs of modules with improved geometries to avoid thermal stresses.

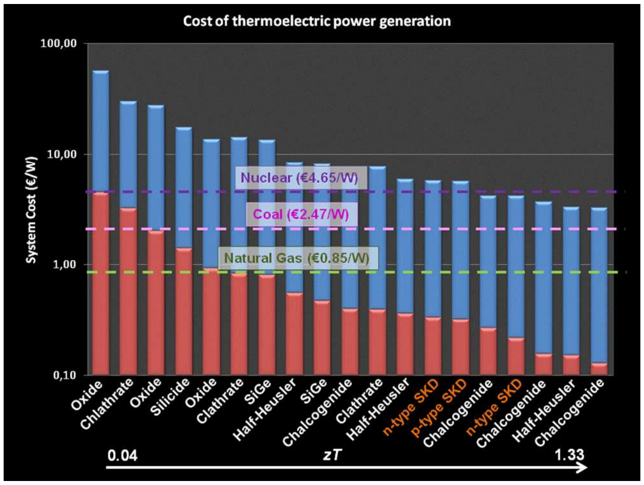

Fig. 7 System cost (€/W) in a logarithm scale of different bulk thermoelectric power generation materials, for a ΔT= 725 K (in the intermediate temperature range). In the x-axis the family name of each compound is written. Red colour represents the basic costs including material costs, efficiency and optimal geometry, and blue colour corresponds to the module design with optimum filling factor, considering other factors as heat exchangers and real manufacturing costs. Horizontal dashed lines represent the costs of electricity generation in technologies using natural gas in green, coal in pink and nuclear in violet (data extracted from [181]).

Conclusions

Skutterudites have generated a high interest among all thermoelectric materials used at intermediate temperatures, due to their remarkable development in last decades. The Figure of Merit for n-type Skutterudites is up to 1.5 at 800K. These values are achieved thanks to an in-depth study of the physical process theory along with an important effort in the experimental development of these materials. Both aspects have contributed to a better understanding of the crystal structure and the filling of fraction limits in the icosahedral voids. The best performance to obtain an improvement in the Figure of Merit for doped and filled Skutterudites by the reduction of the thermal conductivity is based on two principles: disorder in the crystal structure through the introduction of rattlers and modification of the Co and Sb sites, and the generation of defects in the nanoscale and mesoscale through the formation of nanocomposites. New methods of synthesis to produce these materials at large scale with good thermoelectric properties have also been developed.

The best results for the Figure of Merit were obtained for ternary Skutterudites in the beginning of the 90's in the case of p-type Skutterudites and few improvements have been achieved since then. Many efforts must be made in order to further improve these materials.

Finally, it is remarkable that some devices based on these materials have been produced in laboratories, and in the coming years it is expected that commercial thermoelectric devices based on Skutterudites for intermediate temperatures will be available worldwide.

Acknowledgments

The authors acknowledge partial financial support from NEXTEC "Next Generation Nano-engineered Thermoelectric Converters – from concept to industrial validation", project founded by the European Commission under the Seventh Framework Programme (FP7) since July 2011. Grant # 263167.

Notes and references

[a] *IMM-Instituto de Microelectrónica de Madrid (CNM-CSIC), Isaac Newton 8, PTM,E-28760 Tres Cantos,Madrid. Fax:+34 806 0701; Tel:+34 8060 700; E-mail:Marisol@imm.cnm.csic.es*
[b] *Dept. Electrocerámica, Instituto de Cerámica y Vidrio,C/ Kelsen 5, E-28049 Madrid. Tel: 91 735 58 40 E-mail:jfernandez@icv.csic.es*

1. *Real Prospects for Energy Efficiency in the United States*, The National Academies Press, Washington, DC, 2010.
2. J. Yang, Thermoelectrics, 2005. ICT 2005. 24th International Conference on, 2005.
3. L. E. Bell, *Science*, 2008, **321**, 1457-1461.
4. D. M. Rowe, *International Journal of Innovations in Energy Systems and Power*, 2006, **1**, 13-23.
5. G. J. Snyder, *The Electrochemical Society Interface*, 2008, **17**, 54.
6. D. S. Ginley and D. Cahen, *Fundamentals of materials for energy and environmental sustainability*, Cambridge university press, 2011.

7. D. M. Rowe, *Thermoelectrics handbook macro to nano*, CRC/Taylor & Francis, Boca Raton, 2006.
8. E. R. E. Council, *Rethinking 2050*.
9. D.-Y. Chung, T. P. Hogan, M. Rocci-Lane, P. Brazis, J. R. Ireland, C. R. Kannewurf, M. Bastea, C. Uher and M. G. Kanatzidis, *Journal of the American Chemical Society*, 2004, **126**, 6414-6428.
10. G. H. Kim, L. Shao, K. Zhang and K. P. Pipe, *Nat Mater*, 2013, **12**, 719-723.
11. S. I. Kim, K. H. Lee, H. A. Mun, H. S. Kim, S. W. Hwang, J. W. Roh, D. J. Yang, W. H. Shin, X. S. Li, Y. H. Lee, G. J. Snyder and S. W. Kim, *Science*, 2015, **348**, 109-114.
12. P. F. P. Poudeu, J. D'Angelo, A. D. Downey, J. L. Short, T. P. Hogan and M. G. Kanatzidis, *Angewandte Chemie International Edition*, 2006, **45**, 3835-3839.
13. K. Biswas, J. He, I. D. Blum, C.-I. Wu, T. P. Hogan, D. N. Seidman, V. P. Dravid and M. G. Kanatzidis, *Nature*, 2012, **489**, 414-418.
14. E. M. Levin, S. L. Bud'ko and K. Schmidt-Rohr, *Advanced Functional Materials*, 2012, **22**, 2766-2774.
15. T. Caillat, J.-P. Fleurial and A. Borshchevsky, *Journal of Physics and Chemistry of Solids*, 1997, **58**, 1119-1125.
16. J. Sui, J. Li, J. He, Y.-L. Pei, D. Berardan, H. Wu, N. Dragoe, W. Cai and L.-D. Zhao, *Energy & Environmental Science*, 2013, **6**, 2916-2920.
17. H. Liu, X. Shi, F. Xu, L. Zhang, W. Zhang, L. Chen, Q. Li, C. Uher, T. Day and G. J. Snyder, *Nat Mater*, 2012, **11**, 422-425.
18. E. S. Toberer, C. A. Cox, S. R. Brown, T. Ikeda, A. F. May, S. M. Kauzlarich and G. J. Snyder, *Advanced Functional Materials*, 2008, **18**, 2795-2800.
19. X. Yan, W. Liu, H. Wang, S. Chen, J. Shiomi, K. Esfarjani, H. Wang, D. Wang, G. Chen and Z. Ren, *Energy & Environmental Science*, 2012, **5**, 7543-7548.
20. G. Joshi, H. Lee, Y. Lan, X. Wang, G. Zhu, D. Wang, R. W. Gould, D. C. Cuff, M. Y. Tang, M. S. Dresselhaus, G. Chen and Z. Ren, *Nano Letters*, 2008, **8**, 4670-4674.
21. S. Wang, H. Li, R. Lu, G. Zheng and X. Tang, *Nanotechnology*, 2013, **24**, 285702.
22. K. F. Hsu, S. Loo, F. Guo, W. Chen, J. S. Dyck, C. Uher, T. Hogan, E. K. Polychroniadis and M. G. Kanatzidis, *Science*, 2004, **303**, 818-821.
23. W. Liu, X. Tan, K. Yin, H. Liu, X. Tang, J. Shi, Q. Zhang and C. Uher, *Physical Review Letters*, 2012, **108**, 166601.
24. J.-S. Rhyee, K. H. Lee, S. M. Lee, E. Cho, S. I. Kim, E. Lee, Y. S. Kwon, J. H. Shim and G. Kotliar, *Nature*, 2009, **459**, 965-968.
25. Y. Pei, J. Lensch-Falk, E. S. Toberer, D. L. Medlin and G. J. Snyder, *Advanced Functional Materials*, 2011, **21**, 241-249.
26. X. Shi, J. Yang, J. R. Salvador, M. Chi, J. Y. Cho, H. Wang, S. Bai, J. Yang, W. Zhang and L. Chen, *Journal of the American Chemical Society*, 2011, **133**, 7837-7846.
27. A. Saramat, G. Svensson, A. E. C. Palmqvist, C. Stiewe, E. Mueller, D. Platzek, S. G. K. Williams, D. M. Rowe, J. D. Bryan and G. D. Stucky, *J. Appl. Phys.*, 2006, **99**, 023708-023708-023705.
28. X. W. Wang, H. Lee, Y. C. Lan, G. H. Zhu, G. Joshi, D. Z. Wang, J. Yang, A. J. Muto, M. Y. Tang, J. Klatsky, S. Song, M. S. Dresselhaus, G. Chen and Z. F. Ren, *Applied Physics Letters*, 2008, **93**, 193121.
29. A. F. May, J.-P. Fleurial and G. J. Snyder, *Physical Review B*, 2008, **78**, 125205.
30. C. B. Vining, *Nat Mater*, 2009, **8**, 83-85.
31. C. Han, Z. Li and S. Dou, *Chinese Science Bulletin*, 2014, **59**, 2073-2091.
32. *"Voyager Mission Operations Status Reports" Voyager-jpl.nasa.gov web* Retrieved 24 July 2011.
33. V. Zlatic and A. Hewson, *New materials for Thermoelectric Applications: Theory and Experiment*, Springer Netherlands, 2013.
34. D. M. Rowe, V. S. Shukla and N. Savvides, *Nature*, 1981, **290**, 765-766.
35. L. D. Hicks and M. S. Dresselhaus, *Physical Review B*, 1993, **47**, 12727-12731.
36. M. S. Dresselhaus, G. Chen, M. Y. Tang, R. Yang, H. Lee, D. Wang, Z. Ren, J. P. Fleurial and P. Gogna, *Advanced Materials*, 2007, **19**, 1043-1053.
37. J. R. Szczech, J. M. Higgins and S. Jin, *J. Mater. Chem.*, 2011, **21**, 4037-4055.
38. G. A. Slack, *CRC Handbook of Thermoelectrics*, CRC Press, Boca Raton, FL, 1995.
39. G. A. Slack, *Proceedings of the 1992 1st National Thermogenic Cooler Conference*, 1992, 171-195.
40. G. J. Snyder and E. S. Toberer, *Nat Mater*, 2008, **7**, 105-114.
41. T. M. Tritt, *Thermoelectric Materials: New Directions and Approaches : Symposium Held March 31-April 3, 1997, San Francisco, California, USA*, Materials Research Society, 1997.
42. A. Shakouri, *Annual Review of Materials Research*, 2011, **41**, 399-431.
43. M. Martin-Gonzalez, O. Caballero-Calero and P. Diaz-Chao, *Renew. Sust. Energ. Rev.*, 2013, **24**, 288-305.
44. J.-i. Tani and H. Kido, *Intermetallics*, 2007, **15**, 1202-1207.
45. J.-i. Tani and H. Kido, *Physica B: Condensed Matter*, 2005, **364**, 218-224.
46. S. Bhattacharya, A. Bohra, R. Basu, R. Bhatt, S. Ahmad, K. N. Meshram, A. K. Debnath, A. Singh, S. K. Sarkar, M. Navneethan, Y. Hayakawa, D. K. Aswal and S. K. Gupta, *Journal of Materials Chemistry A*, 2014, **2**, 17122-17129.
47. D. Brown, T. Day, T. Caillat and G. J. Snyder, *Journal of Elec Materi*, 2013, **42**, 2014-2019.
48. *DIRECTIVE 2002/95/EC OF THE EUROPEAN PARLIAMENT AND OF THE COUNCIL of 27 January 2003 on the restriction of the use of certain hazardous substances in electrical and electronic equipment.*
49. *COMMISSION DIRECTIVE 2011/37/EU of 30 March 2011amending Annex II to Directive 2000/53/EC of the European Parliament and of the Council on end-of-life vehicles.*
50. Y. Moelo, E. Makovicky, N. N. Mozgova, J. L. Jambor, N. Cook, A. Pring, W. Paar, E. H. Nickel, S. Graeser, S. Karup-Moller, T. Balic-Zunic, W. G. Mumme, F. Vurro, D. Topa, L. Bindi, K. Bente and M. Shimizu, *European Journal of Mineralogy*, 2008, **20**, 7-46.
51. H. Dittrich, A. Stadler, D. Topa, H. J. Schimper and A. Basch, *physica status solidi (a)*, 2009, **206**, 1034-1041.
52. J. Heo, G. Laurita, S. Muir, M. A. Subramanian and D. A. Keszler, *Chemistry of Materials*, 2014, **26**, 2047-2051.
53. K. Suekuni, K. Tsuruta, M. Kunii, H. Nishiate, E. Nishibori, S. Maki, M. Ohta, A. Yamamoto and M. Koyano, *J. Appl. Phys.*, 2013, **113**, 043712.
54. I. Oftedal, in *Zeitschrift für Kristallographie - Crystalline Materials*, 1928, vol. 66, p. 517.
55. A. Kjekshus and T. Rakke, *Acta Chem. Scand. A*, 1974, **28**, 99-103.

56. C. Uher, in *Semiconductors and Semimetals*, ed. M. T. Terry, Elsevier, 2001, vol. Volume 69, pp. 139-253.
57. T. Caillat, J. P. Fleurial and A. Borshchevsky, *Journal of Crystal Growth*, 1996, **166**, 722-726.
58. D. T. Morelli, T. Caillat, J. P. Fleurial, A. Borshchevsky, J. Vandersande, B. Chen and C. Uher, *Physical Review B*, 1995, **51**, 9622-9628.
59. L. Bertini, K. Biliquist, M. Christensen, C. Gatti, L. Holmgren, B. Iversen, E. Mueller, M. Muhammed, G. Noriega, A. Palmqvist, D. Platzek, D. M. Rowe, A. Saramat, C. Stiewe, M. Toprak, S. G. Williams and Y. Zhang, Thermoelectrics, 2003 Twenty-Second International Conference on - ICT, 2003.
60. J. X. Zhang, Q. M. Lu, K. G. Liu, L. Zhang and M. L. Zhou, *Materials Letters*, 2004, **58**, 1981-1984.
61. W.-S. Liu, B.-P. Zhang, J.-F. Li and L.-D. Zhao, *Journal of Physics D: Applied Physics*, 2007, **40**, 6784.
62. C.-H. Park and Y.-S. Kim, *Physical Review B*, 2010, **81**, 085206.
63. S. Bhattacharya and R. Mallik, *Journal of Elec Materi*, 2011, **40**, 1221-1232.
64. Y. Kawaharada, K. Kurosaki, M. Uno and S. Yamanaka, *Journal of Alloys and Compounds*, 2001, **315**, 193-197.
65. G. A. Slack and V. G. Tsoukala, *J. Appl. Phys.*, 1994, **76**, 1665-1671.
66. G. S. Nolas, J. L. Cohn and G. A. Slack, *Physical Review B*, 1998, **58**, 164-170.
67. V. Keppens, D. Mandrus, B. C. Sales, B. C. Chakoumakos, P. Dai, R. Coldea, M. B. Maple, D. A. Gajewski, E. J. Freeman and S. Bennington, *Nature*, 1998, **395**, 876-878.
68. R. P. Hermann, R. Jin, W. Schweika, F. Grandjean, D. Mandrus, B. C. Sales and G. J. Long, *Physical Review Letters*, 2003, **90**, 135505.
69. J. Feldman and D. Singh, *Physical Review B*, 1996, **53**, 6273-6282.
70. M. M. Koza, M. R. Johnson, R. Viennois, H. Mutka, L. Girard and D. Ravot, *Nature Materials*, 2008, **7**, 805-810.
71. W. Li and N. Mingo, *Physical Review B*, 2014, **89**, 184304.
72. W. Jeitschko and D. Braun, *Acta Crystallographica Section B*, 1977, **33**, 3401-3406.
73. B. C. Sales, D. Mandrus and R. K. Williams, *Science*, 1996, **272**, 1325-1328.
74. B. C. Sales, D. Mandrus, B. C. Chakoumakos, V. Keppens and J. R. Thompson, *Physical Review B*, 1997, **56**, 15081-15089.
75. J. P. Fleurial, A. Borshchevsky, T. Caillat, D. T. Morelli and G. P. Meisner, Thermoelectrics, 1996., Fifteenth International Conference on, 1996.
76. L. Chen, Thermoelectrics, 2002. Proceedings ICT '02. Twenty-First International Conference on, 2002.
77. X. Shi, S. Bai, L. Xi, J. Yang, W. Zhang, L. Chen and J. Yang, *Journal of Materials Research*, 2011, **26**, 1745-1754.
78. J. Yang, W. Zhang, S. Q. Bai, Z. Mei and L. D. Chen, *Applied Physics Letters*, 2007, **90**, -.
79. Y. Z. Pei, S. Q. Bai, X. Y. Zhao, W. Zhang and L. D. Chen, *Solid State Sciences*, 2008, **10**, 1422-1428.
80. Y. Z. Pei, J. Yang, L. D. Chen, W. Zhang, J. R. Salvador and J. Yang, *Applied Physics Letters*, 2009, **95**, 042101.
81. Y. Z. Pei, L. D. Chen, W. Zhang, X. Shi, S. Q. Bai, X. Y. Zhao, Z. G. Mei and X. Y. Li, *Applied Physics Letters*, 2006, **89**, 221107.
82. J. Zhang, B. Xu, L.-M. Wang, D. Yu, J. Yang, F. Yu, Z. Liu, J. He, B. Wen and Y. Tian, *Acta Materialia*, 2012, **60**, 1246-1251.
83. L. D. Chen, T. Kawahara, X. F. Tang, T. Goto, T. Hirai, J. S. Dyck, W. Chen and C. Uher, *J. Appl. Phys.*, 2001, **90**, 1864-1868.
84. M. Puyet, B. Lenoir, A. Dauscher, M. Dehmas, C. Stiewe and E. Muller, *J. Appl. Phys.*, 2004, **95**, 4852-4855.
85. X. Y. Zhao, X. Shi, L. D. Chen, W. Q. Zhang, W. B. Zhang and Y. Z. Pei, *J. Appl. Phys.*, 2006, **99**, 053711.
86. Q. M. Lu, J. X. Zhang, X. Zhang, Y. Q. Liu, D. M. Liu and M. L. Zhou, *J. Appl. Phys.*, 2005, **98**, 106107.
87. G. Rogl, Z. Aabdin, E. Schafler, J. Horky, D. Setman, M. Zehetbauer, M. Kriegisch, O. Eibl, A. Grytsiv, E. Bauer, M. Reinecker, W. Schranz and P. Rogl, *Journal of Alloys and Compounds*, 2012, **537**, 183-189.
88. G. Rogl, A. Grytsiv, P. Rogl, N. Peranio, E. Bauer, M. Zehetbauer and O. Eibl, *Acta Materialia*, 2014, **63**, 30-43.
89. W. Zhao, P. Wei, Q. Zhang, C. Dong, L. Liu and X. Tang, *Journal of the American Chemical Society*, 2009, **131**, 3713-3720.
90. X. Shi, H. Kong, C.-P. Li, C. Uher, J. Yang, J. R. Salvador, H. Wang, L. Chen and W. Zhang, *Applied Physics Letters*, 2008, **92**, -.
91. W.-S. Liu, B.-P. Zhang, L.-D. Zhao and J.-F. Li, *Chemistry of Materials*, 2008, **20**, 7526-7531.
92. J. R. Sootsman, D. Y. Chung and M. G. Kanatzidis, *Angewandte Chemie International Edition*, 2009, **48**, 8616-8639.
93. H. Anno, K. Matsubara, Y. Notohara, T. Sakakibara and H. Tashiro, *J. Appl. Phys.*, 1999, **86**, 3780-3786.
94. L. Bertini, C. Stiewe, M. Toprak, S. Williams, D. Platzek, A. Mrotzek, Y. Zhang, C. Gatti, E. Muller, M. Muhammed and M. Rowe, *J. Appl. Phys.*, 2003, **93**, 438-447.
95. H. Tashiro, Y. Notohara, T. Sakakibara, H. Anno and K. Matsubara, in *International Conference on Thermoelectrics*, 1997, pp. 326-329.
96. Q. He, S. Hu, X. Tang, Y. Lan, J. Yang, X. Wang, Z. Ren, Q. Hao and G. Chen, *Applied Physics Letters*, 2008, **93**, 042108.
97. I. Dimitrov, M. Manley, S. Shapiro, J. Yang, W. Zhang, L. Chen, Q. Jie, G. Ehlers, A. Podlesnyak, J. Camacho and Q. Li, *Physical Review B*, 2010, **82**, 174301.
98. W.-S. Liu, B.-P. Zhang, J.-F. Li, H.-L. Zhang and L.-D. Zhao, *J. Appl. Phys.*, 2007, **102**, -.
99. B. Duan, P. Zhai, L. Liu, Q. Zhang and X. Ruan, *J Mater Sci: Mater Electron*, 2012, **23**, 1817-1822.
100. X. Su, H. Li, G. Wang, H. Chi, X. Zhou, X. Tang, Q. Zhang and C. Uher, *Chemistry of Materials*, 2011, **23**, 2948-2955.
101. R. C. Mallik, R. Anbalagan, G. Rogl, E. Royanian, P. Heinrich, E. Bauer, P. Rogl and S. Suwas, *Acta Materialia*, 2013, **61**, 6698-6711.
102. L. Bertini, G. Borot, K. Billquist, M. Christensen, C. Gatti, L. Holmgren, B. Iversen, E. Mueller, M. Muhammed, G. Noriega, A. Palmqvist, D. Platzek, D. M. Rowe, A. Saramat, C. Stiewe, M. Toprak, S. G. Williams and Y. Zhang, Thermoelectrics, 2003 Twenty-Second International Conference on - ICT, 2003.
103. C. Stiewe, L. Bertini, M. Toprak, M. Christensen, D. Platzek, S. Williams, C. Gatti, E. Müller, B. B. Iversen, M. Muhammed and M. Rowe, *J. Appl. Phys.*, 2005, **97**, -.
104. M. Chitroub, F. Besse and H. Scherrer, *Journal of Alloys and Compounds*, 2009, **467**, 31-34.
105. C. Xu, B. Duan, S. Ding, P. Zhai and Q. Zhang, *Journal of Elec Materi*, 2014, **43**, 2224-2228.
106. J. S. Dyck, W. Chen, C. Uher, L. Chen, X. Tang and T. Hirai, *J. Appl. Phys.*, 2002, **91**, 3698-3705.
107. M. Puyet, A. Dauscher, B. Lenoir, C. Bellouard, C. Stiewe, E. Müller, J. Hejtmanek and J. Tobola, *Physical Review B*, 2007, **75**, 245110.

108.G. Rogl, A. Grytsiv, E. Bauer, P. Rogl and M. Zehetbauer, *Intermetallics*, 2010, **18**, 394-398.

109.X. Zhang, Q. M. Lu, J. X. Zhang, Q. Wei, D. M. Liu and Y. Q. Liu, *Journal of Alloys and Compounds*, 2008, **457**, 368-371.

110.X. Y. Li, L. D. Chen, J. F. Fan, W. B. Zhang, T. Kawahara and T. Hirai, *J. Appl. Phys.*, 2005, **98**, 083702.

111.T. Liang, X. Su, Y. Yan, G. Zheng, Q. Zhang, H. Chi, X. Tang and C. Uher, *J. Mater. Chem. A*, 2014, **2**, 17914-17918.

112.R. C. Mallik, J.-Y. Jung, S.-C. Ur and I.-H. Kim, *Metals and Materials International*, 2008, **14**, 615-620.

113.S. Katsuyama, Y. Shichijo, M. Ito, K. Majima and H. Nagai, *J. Appl. Phys.*, 1998, **84**, 6708-6712.

114.A. A. Ioannidou, M. Rull, M. Martin-Gonzalez, A. Moure, A. Jacquot and D. Niarchos, *Journal of Elec Materi*, 2014, **43**, 2637-2643.

115.D. T. Morelli and G. P. Meisner, *J. Appl. Phys.*, 1995, **77**, 3777-3781.

116.X. Tang, Q. Zhang, L. Chen, T. Goto and T. Hirai, *J. Appl. Phys.*, 2005, **97**, 093712.

117.R. Mallik, R. Anbalagan, K. Raut, A. Bali, E. Royanian, E. Bauer, G. Rogl and P. Rogl, *Journal of Physics: Condensed Matter*, 2013, **25**, 105701.

118.J. Yang, R. Liu, Z. Chen, L. Xi, J. Yang, W. Zhang and L. Chen, *Applied Physics Letters*, 2012, **101**, 022101.

119.J. Yang, S. Wang, J. Yang, W. Zhang and L. Chen, *MRS Online Proceedings Library*, 2013, **1490**, 9-18.

120.L. Zhang, A. Grytsiv, M. Kerber, P. Rogl, E. Bauer and M. Zehetbauer, *Journal of Alloys and Compounds*, 2010, **490**, 19-25.

121.G. Rogl, A. Grytsiv, E. Bauer, P. Rogl and M. Zehetbauer, *Intermetallics*, 2010, **18**, 57-64.

122.G. Rogl, A. Grytsiv, P. Heinrich, E. Bauer, P. Kumar, N. Peranio, O. Eibl, J. Horky, M. Zehetbauer and P. Rogl, *Acta Materialia*, 2015, **91**, 227-238.

123.G. Rogl, A. Grytsiv, P. Rogl, E. Bauer, M. B. Kerber, M. Zehetbauer and S. Puchegger, *Intermetallics*, 2010, **18**, 2435-2444.

124.X. F. Tang, L. D. Chen, T. Goto, T. Hirai and R. Z. Yuan, *Journal of Materials Science*, 2001, **36**, 5435-5439.

125.P. F. Qiu, J. Yang, R. H. Liu, X. Shi, X. Y. Huang, G. J. Snyder, W. Zhang and L. D. Chen, *J. Appl. Phys.*, 2011, **109**, 063713.

126.L. Zhou, P. Qiu, C. Uher, X. Shi and L. Chen, *Intermetallics*, 2013, **32**, 209-213.

127.G. Rogl, A. Grytsiv, P. Rogl, E. Bauer and M. Zehetbauer, *Intermetallics*, 2011, **19**, 546-555.

128.Z. He, C. Stiewe, D. Platzek, G. Karpinski, E. Müller, S. Li, M. Toprak and M. Muhammed, *Nanotechnology*, 2007, **18**, 235602.

129.C. Chubilleau, B. Lenoir, A. Dauscher and C. Godart, *Intermetallics*, 2012, **22**, 47-54.

130.X. Shi, L. Chen, J. Yang and G. P. Meisner, *Applied Physics Letters*, 2004, **84**, 2301-2303.

131.E. Alleno, L. Chen, C. Chubilleau, B. Lenoir, O. Rouleau, M. F. Trichet and B. Villeroy, *Journal of Elec Materi*, 2010, **39**, 1966-1970.

132.L. Fu, J. Yang, J. Peng, Q. Jiang, Y. Xiao, Y. Luo, D. Zhang, Z. Zhou, M. Zhang, Y. Cheng and F. Cheng, *Journal of Materials Chemistry A*, 2015.

133.H. Li, X. Tang, Q. Zhang and C. Uher, *Applied Physics Letters*, 2009, **94**, 102114.

134.H. Li, X. Tang, X. Su and Q. Zhang, *Applied Physics Letters*, 2008, **92**, -.

135.X. Y. Zhao, X. Shi, L. D. Chen, W. Q. Zhang, S. Q. Bai, Y. Z. Pei, X. Y. Li and T. Goto, *Applied Physics Letters*, 2006, **89**, 092121.

136.Z. Xiong, X. Chen, X. Huang, S. Bai and L. Chen, *Acta Materialia*, 2010, **58**, 3995-4002.

137.X. J. Zheng, L. Zhu, Y.-H. Zhou and Q. Zhang, *Applied Physics Letters*, 2005, **87**, -.

138.M. S. Toprak, C. Stiewe, D. Platzek, S. Williams, L. Bertini, E. Müller, C. Gatti, Y. Zhang, M. Rowe and M. Muhammed, *Advanced Functional Materials*, 2004, **14**, 1189-1196.

139.X. Shi, H. Kong, C.-P. Li, C. Uher, J. Yang, J. R. Salvador, H. Wang, L. Chen and W. Zhang, *Applied Physics Letters*, 2008, **92**, 182101.

140.H. Li, X. Tang, Q. Zhang and C. Uher, *Applied Physics Letters*, 2008, **93**, 252109.

141.Q. Li, Z. Lin and J. Zhou, *Journal of Elec Materi*, 2009, **38**, 1268-1272.

142.G. Tan, W. Liu, S. Wang, Y. Yan, H. Li, X. Tang and C. Uher, *Journal of Materials Chemistry A*, 2013, **1**, 12657-12668.

143.K. Biswas, S. Muir and M. A. Subramanian, *Materials Research Bulletin*, 2011, **46**, 2288-2290.

144.P. Baláz, *Mechanochemistry in Nanoscience and Minerals Engineering*, Springer-Verlag, Heidelberg, 2008.

145.J. Yang, Y. Chen, J. Peng, X. Song, W. Zhu, J. Su and R. Chen, *Journal of Alloys and Compounds*, 2004, **375**, 229-232.

146.W.-S. Liu, B.-P. Zhang, J.-F. Li and L.-D. Zhao, *Journal of Physics D: Applied Physics*, 2007, **40**, 566.

147.J. Peng, J. Yang, T. Zhang, X. Song and Y. Chen, *Journal of Alloys and Compounds*, 2004, **381**, 313-316.

148.J. L. Mi, T. J. Zhu, X. B. Zhao and J. Ma, *J. Appl. Phys.*, 2007, **101**, 054314.

149.G. Rogl, D. Setman, E. Schafler, J. Horky, M. Kerber, M. Zehetbauer, M. Falmbigl, P. Rogl, E. Royanian and E. Bauer, *Acta Materialia*, 2012, **60**, 2146-2157.

150.G. Rogl, A. Grytsiv, P. Rogl, E. Bauer, M. Hochenhofer, R. Anbalagan, R. C. Mallik and E. Schafler, *Acta Materialia*, 2014, **76**, 434-448.

151.J. Eilertsen, R. Berthelot, A. W. Sleight and M. Subramanian, *Journal of Solid State Chemistry*, 2012, **190**, 238-245.

152.X. Shi, Z. Zhou, W. Zhang, L. D. Chen, J. Yang and C. Uher, *J. Appl. Phys.*, 2007, **101**, 123525.

153.J. Yang, L. Zhang, Y. Liu, C. Chen, J. Li, D. Yu, J. He, Z. Liu, Y. Tian and B. Xu, *J. Appl. Phys.*, 2013, **113**, 113703.

154.X. Li, B. Xu, L. Zhang, F. Duan, X. Yan, J. Yang and Y. Tian, *Journal of Alloys and Compounds*, 2014, **615**, 177-180.

155.D. M. Rowe and G. Min, *Journal of Power Sources*, 1998, **73**, 193-198.

156.S. Wan, X. Huang, P. Qiu, S. Bai and L. Chen, *Materials & Design*, 2015, **67**, 379-384.

157.B. Duan, P. Zhai, P. Wen, S. Zhang, L. Liu and Q. Zhang, *Scripta Materialia*, 2012, **67**, 372-375.

158.J. R. Salvador, R. A. Waldo, C. A. Wong, M. Tessema, D. N. Brown, D. J. Miller, H. Wang, A. A. Wereszczak and W. Cai, *Materials Science and Engineering: B*, 2013, **178**, 1087-1096.

159.J. R. Salvador, J. Y. Cho, Z. Ye, J. E. Moczygemba, A. J. Thompson, J. W. Sharp, J. D. Koenig, R. Maloney, T. Thompson, J. Sakamoto, H. Wang and A. A. Wereszczak, *Physical Chemistry Chemical Physics*, 2014, **16**, 12510-12520.

160. G. Rogl, L. Zhang, P. Rogl, A. Grytsiv, M. Falmbigl, D. Rajs, M. Kriegisch, H. Müller, E. Bauer, J. Koppensteiner, W. Schranz, M. Zehetbauer, Z. Henkie and M. B. Maple, *J. Appl. Phys.*, 2010, **107**, -.
161. K. T. Wojciechowski, R. Zybala and R. Mania, *Microelectronics Reliability*, 2011, **51**, 1198-1202.
162. D. Zhao, X. Li, L. He, W. Jiang and L. Chen, *Intermetallics*, 2009, **17**, 136-141.
163. H. Xia, F. Drymiotis, C.-L. Chen, A. Wu and G. J. Snyder, *Journal of Materials Science*, 2014, **49**, 1716-1723.
164. D. Zhao, H. Geng and X. Teng, *Journal of Alloys and Compounds*, 2012, **517**, 198-203.
165. D. Zhao, C. Tian, Y. Liu, C. Zhan and L. Chen, *Journal of Alloys and Compounds*, 2011, **509**, 3166-3171.
166. C. T. Snyder GJ, February 17-20, 2004.
167. J. Leszczynski, K. Wojciechowski and A. Malecki, *J Therm Anal Calorim*, 2011, **105**, 211-222.
168. R. Hara, S. Inoue, H. T. Kaibe and S. Sano, *Journal of Alloys and Compounds*, 2003, **349**, 297-301.
169. D. Zhao, C. Tian, S. Tang, Y. Liu and L. Chen, *Journal of Alloys and Compounds*, 2010, **504**, 552-558.
170. E. Godlewska, K. Zawadzka, A. Adamczyk, M. Mitoraj and K. Mars, *Oxid Met*, 2010, **74**, 113-124.
171. G. Skomedal, N. R. Kristiansen, M. Engvoll and H. Middleton, *Journal of Elec Materi*, 2013, 1-6.
172. X. Xia, X. Huang, X. Li, M. Gu, P. Qiu, J. Liao, Y. Tang, S. Bai and L. Chen, *Journal of Alloys and Compounds*, 2014, **604**, 94-99.
173. H. Dong, X. Li, X. Huang, Y. Zhou, W. Jiang and L. Chen, *Ceramics International*, 2013, **39**, 4551-4557.
174. H. Dong, X. Li, Y. Tang, J. Zou, X. Huang, Y. Zhou, W. Jiang, G.-j. Zhang and L. Chen, *Journal of Alloys and Compounds*, 2012, **527**, 247-251.
175. M. Kambe, T. Jinushi and Z. Ishijima, *Journal of Elec Materi*, 2014, **43**, 1959-1965.
176. J. S. Sakamoto, H. Schock, T. Caillat, J. P. Fleurial, R. Maloney, M. Lyle, T. Ruckle, E. Timm and L. Zhang, *Science of Advanced Materials*, 2011, **3**, 621-632.
177. E. Alleno, N. Lamquembe, R. Cardoso-Gil, M. Ikeda, F. Widder, O. Rouleau, C. Godart, Y. Grin and S. Paschen, *physica status solidi (a)*, 2014, **211**, 1293-1300.
178. S. A. Omer and D. G. Infield, *Solar Energy Materials and Solar Cells*, 1998, **53**, 67-82.
179. S. K. Yee, S. LeBlanc, K. E. Goodson and C. Dames, *Energy & Environmental Science*, 2013, **6**, 2561-2571.
180. K. Yazawa and A. Shakouri, *Environmental Science & Technology*, 2011, **45**, 7548-7553.
181. S. LeBlanc, S. K. Yee, M. L. Scullin, C. Dames and K. E. Goodson, *Renewable and Sustainable Energy Reviews*, 2014, **32**, 313-327.